

How to characterize the dynamics of cold atoms in non-dissipative optical lattices?

D. Hennequin and Ph. Verkerk

Phil. Trans. R. Soc. A 2010 **368**, 2163-2177

doi: 10.1098/rsta.2010.0027

References

[This article cites 25 articles](#)

<http://rsta.royalsocietypublishing.org/content/368/1918/2163.full.html#ref-list-1>

Rapid response

[Respond to this article](#)

<http://rsta.royalsocietypublishing.org/letters/submit/roypta;368/1918/2163>

Subject collections

Articles on similar topics can be found in the following collections

[atomic and molecular physics](#) (4 articles)

Email alerting service

Receive free email alerts when new articles cite this article - sign up in the box at the top right-hand corner of the article or click [here](#)

To subscribe to *Phil. Trans. R. Soc. A* go to:

<http://rsta.royalsocietypublishing.org/subscriptions>

How to characterize the dynamics of cold atoms in non-dissipative optical lattices?

BY D. HENNEQUIN* AND PH. VERKERK

*Laboratoire PhLAM, UMR CNRS, CERLA, Université de Lille 1,
59655 Villeneuve d'Ascq, France*

We examine here the classical dynamics of cold atoms in square optical lattices, i.e. lattices obtained with two orthogonal stationary plane waves. Contrary to many of the past studies in this domain, the potential here is time independent and non-dissipative. We show that, as a function of the experimental parameters, very different behaviours are obtained, both for the dynamics of atoms trapped inside individual sites and for atoms travelling between sites: inside the sites, chaos may be the main regime or, on the contrary, it may be negligible; outside the sites, chaos sometimes coexists with other regimes. We discuss the consequences of these differences on the macroscopic behaviour of the atoms in the lattice, and we propose experimental measurements able to characterize these dynamics and to distinguish between the different cases.

Keywords: cold atom; chaos; optical lattice; nonlinear dynamics

1. Introduction

The cooling of atoms to extremely low temperatures, through the use of magneto-optical traps (MOTs), has provided since the mid-1980s fantastic possibilities to increase our experimental knowledge of the quantum world. The most spectacular of these was the achievement of the Bose–Einstein condensation, and thus of macroscopic quantum objects. However, even in the classical world, the possibility of studying the dynamics of atoms not ‘blurred’ by the Doppler effect is very exciting. This requires the development of tools to manipulate the atoms, e.g. for guiding them or ‘designing’ their phase space.

Optical lattices provide such tools; their versatility allows atoms to be manipulated with an extreme precision and a relative ease (Guidoni & Verkerk 1999). Because of these qualities, they represent an outstanding toy model, and have recently attracted increasing interest in various domains. Condensed matter systems and strongly correlated cold atoms in optical lattices have strong similarities, as in the superfluid–Mott insulator quantum phase transition (Greiner *et al.* 2002) or in the Tonks–Girardeau regime (Paredes *et al.* 2004). Here, the interactions between atoms play a crucial role, and require the use of a Bose–Einstein condensate. In particular, instabilities are expected in the Gross–Pitaevskii equation because of the nonlinear term (Thommen *et al.* 2003;

*Author for correspondence (daniel.hennequin@univ-lille1.fr).

Fang & Hai 2005; Kuan *et al.* 2007). Quantum computing also requires a coupling between atoms; the optical lattices appear to be an efficient implementation of a Feynman's universal quantum simulator (Jaksch & Zoller 2005), and are among the most promising candidates for the realization of a quantum computer (Mandel *et al.* 2003; Vollbrecht *et al.* 2004). On the other hand, non-interacting atoms also exhibit interesting behaviours. In this case, the physics is essentially that of a single atom. A higher number of atoms simply increases the observable signal. That is the case in statistical physics, where cold atoms in optical lattices, through their tunability, made possible the observation of the transition between Gaussian and power-law tail distributions, in particular the Tsallis distributions (Jersblad *et al.* 2004; Douglas *et al.* 2006) or that of Anderson localization (Billy *et al.* 2008; Chabé *et al.* 2008; Roati *et al.* 2008).

Non-interacting cold atoms also appear to be an ideal model system to study the dynamics of a system in its classical and quantum limits. Both are closely related, as the latter is defined only as a function of the former. In particular, quantum chaos is defined as the quantum regime of a system whose classical dynamics is chaotic. A good understanding of the classical dynamics is therefore an essential prerequisite to the study of quantum dynamics. In non-dissipative optical lattices, both the classical and the quantum limits are experimentally accessible, and it is even possible to change quasi-continuously from one regime to the other (Steck *et al.* 2000). Moreover, the extreme flexibility of the optical lattices makes it possible to imagine a practically infinite number of configurations by varying the complexity of the lattice and the degree of coupling between the atoms and the lattice.

Many results have been obtained in recent years in the field of quantum chaos (Steck *et al.* 2000; Lignier *et al.* 2005). However, all these studies have used very simple potentials, mainly one-dimensional. Chaos is obtained only with a periodic (or quasi-periodic) temporal forcing of the depth of the lattice (Steck *et al.* 2000; Lignier *et al.* 2005), and only the temporal dynamics of the individual atoms is studied. The introduction of this external clock and the restriction to one-dimensional potentials reduce considerably the generality of these results and the type of possible dynamics. In particular, the behaviours related to the appearance of new frequencies or to a frequency shift (quasi-periodic and homoclinic bifurcations, for example) are impossible.

If we want to overcome these limitations, several problems have to be examined. What type of time-independent lattice will lead to a reasonably complex dynamics? What are the relevant quantities to characterize this dynamics? And what are those that can be implemented experimentally? Note that these questions need to be answered first for the classical atoms. We have to search for a configuration leading to complex classical dynamics. And, experimentally, the dynamics in the classical limit must be characterized before considering the quantum system. In this paper, we address these questions, limiting our analysis to the classical limit. The quantum counterpart will be discussed in a future publication. In §2, we give some facts about cold atoms and optical lattices for those who are not familiar with this domain, and we discuss the possible lattices leading to complex dynamics. Section 3 is devoted to the dynamics of atoms inside the wells, while §4 deals with the dynamics of atoms travelling between several wells. Finally, we discuss in §5 the possible implementation of experimental measurements.

2. Context: cold atoms and optical lattices

Cold atoms refer here to atoms cooled through an MOT. The cooling is mainly obtained through an exchange of the momentum between an atom and a counterpropagating optical beam—while the absorption of a photon by the atom leads to a deceleration of the atom in the direction of the beam, the spontaneous re-emission of the photon arises in a random direction, and so does not change, on average, the atom velocity. To slow down atoms in three dimensions, three pairs of counterpropagating laser beams are necessary. Obviously, a moving atom is decelerated by the photons travelling in the opposite direction, but it is accelerated by photons travelling in the same direction. However, the frequency of these trap beams is detuned to the red of the atomic transition, so that, because of the Doppler effect, the front photons are closer to resonance, and thus the deceleration process is more efficient than the acceleration one. This Doppler cooling process is coupled to an inhomogeneous magnetic field, which enhances the cooling process through the Zeeman level splitting, and adds a restoring force to increase the atomic density of the cloud of cold atoms. MOTs lead typically, for caesium atoms, to a 2 mm diameter cloud of 10^8 atoms at 5 μ K. Such a cloud of cold atoms can exhibit spatio-temporal instabilities and chaos (Wilkowski *et al.* 2000; di Stefano *et al.* 2003, 2004; Hennequin 2004), but an adequate choice of the experimental parameters leads to a stable cloud with atoms whose residual motion is the thermal agitation.

A classical atom follows the motion equations of any classical object, and in particular Newton's second law $F = m\ddot{r}$, where F is the force, r the position and m the mass (in the following, we take $m = 1$). When such an atom is dropped in a stationary wave, it undergoes a force F , the potential U of which is proportional to the wave intensity I , and inversely proportional to the detuning Δ between the wave frequency and the atomic transition frequency,

$$F = -\nabla U \quad (2.1)$$

and

$$U \propto \frac{I}{\Delta}. \quad (2.2)$$

Thus, atoms accumulate in bright (resp. dark) sites for $\Delta < 0$ (resp. $\Delta > 0$). When the atoms are cooled with the MOT, the atomic density in these optical lattices is small enough to neglect the collisions between atoms, and so the only source of dissipation is the spontaneous emission. As spontaneous emission is proportional to I/Δ^2 , it is relatively easy to build conservative optical lattices. Moreover, the classical or quantum nature of the atoms in the lattice can be adjusted continuously, as it depends on the ratio between the temperature (or energy) of the atoms and the depth of the lattice wells. For wells deep enough when compared with the atom temperature, the quantum properties of the atom, and in particular tunnelling, vanish, and thus atoms can be considered as classical (Greiner *et al.* 2001). In the following, we always consider classical atoms, as discussed earlier.

The atom dynamics in the lattice depends on the dimensionality of the lattice. For example, in a one-dimensional lattice, atoms have only two dynamical degrees of freedom, and thus, even if the potential is not harmonic, the dynamics cannot

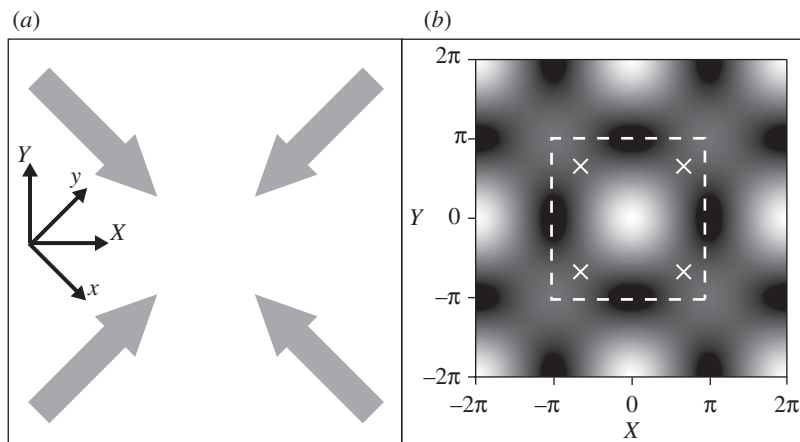


Figure 1. (a) Layout of the laser beams. (b) Spatial distribution of the intensity in the (X, Y) space. Black corresponds to the minimum value (zero intensity), while white corresponds to the maximum. The dotted square delimits the elementary mesh of the lattice, and the white crosses are the saddle points.

be complex. It is necessary to add at least a periodic forcing in such a lattice to observe chaos. On the contrary, a two-dimensional lattice can exhibit chaos, without external forcing.

But the atom dynamics also depends on the lattice geometry, and numerous lattice geometries can be obtained, as, for example, a vertical stack of ring traps (Courtade *et al.* 2006), a fivefold symmetric lattice (Guidoni *et al.* 1999) or even quasi-periodic lattices (Guidoni *et al.* 1997). In this paper, we will focus on the case of two orthogonal stationary plane waves with the same polarization. The configuration of the laser beams is shown in figure 1a. The total field is $\mathcal{E} = \cos kx + e^{i\phi} \sin ky$, where x and y are the two space coordinates, ϕ a phase, $k = 2\pi/\lambda$ the wave vector and λ the wavelength of the laser beam. The intensity can be written as

$$I = \cos^2 kx + \cos^2 ky + 2\alpha \cos kx \cos ky, \quad (2.3)$$

where $\alpha = \cos \phi$. With the adequate normalization, the potential is

$$U_{\pm} = \pm I, \quad (2.4)$$

where the explicit sign is that of Δ . When $\alpha = 0$, the coupling between x and y disappears, and the problem becomes separable. In all the other cases, the coupling between x and y could induce complex dynamics. It is easy to see that, in these cases, the elementary mesh of the potential is on a $\pi/4$ from the (x, y) -axes; thus, it is natural to introduce the following new coordinates:

$$X = kx + ky \quad (2.5)$$

and

$$Y = ky - kx. \quad (2.6)$$

The intensity and the potential can now be written as

$$I = U_+ = -U_- = 1 + \alpha(\cos X + \cos Y) + \cos X \cos Y. \quad (2.7)$$

Before studying the potential, let us concentrate on the intensity. As an example, figure 1*b* shows the spatial distribution of the intensity for $\alpha = 0.5$. The elementary mesh is indicated by the dotted line. Assuming $\alpha > 0$, the intensity I has an absolute maximum $2(1 + \alpha)$ at coordinates $(n2\pi, m2\pi)$, where m and n are integers. It also has a relative maximum $2(1 - \alpha)$ in $(\pi + n2\pi, \pi + m2\pi)$. Once again, we see that $\alpha = 0$ is a special case because the absolute and relative maxima have the same height. Note that $\alpha = 1$ is another special case, where the intensity at the relative maximum vanishes and, thus, is equal to the minimum value. In this special case, we have black lines along $X = \pi + n2\pi$ and $Y = \pi + n2\pi$. We will not consider these cases in the following. On the other hand, the intensity goes to zero in $(\pi + n2\pi, m2\pi)$ and $(n2\pi, \pi + m2\pi)$. Two neighbouring zeros are separated by a saddle point where the intensity has the value $I = 1 - \alpha^2$. It is important to note that these saddle points are on the bisectors, connecting on a straight line an absolute maximum to a relative one and again to the next absolute maximum. On the contrary, the saddle points do not stand on the straight line that connects two neighbouring zeros. This will induce a huge difference in the dynamics of atoms in the lattice obtained for red detunings ($\Delta < 0$), where the atoms are attracted in high-intensity regions, and that for blue detunings ($\Delta > 0$), where the atoms are repelled from these same regions. The bisectors are clearly escape lines for the atoms when $\Delta < 0$, whereas this is not the case for $\Delta > 0$.

Optical lattices appear to be an exciting tool to study the dynamics of a conservative complex system, but how do we characterize this dynamics in the experiments? What are the experimentally accessible quantities? The typical size of a lattice mesh is $\lambda/2$, i.e. 426 nm for caesium. As the diameter of a cold atom cloud is typically 2 mm, the 10^8 atoms are dropped in 22×10^6 sites for a two-dimensional lattice, which leads to five atoms/site. At these scales, it is clear that there is no way to isolate an atom, and thus no way to follow its trajectory. Moreover, to see an atom, we need light, and thus the measure introduces a dissipation and destroys the atomic state. A typical measure consists of illuminating the atoms with a laser flash and recording the fluorescence of the atoms through a camera. This destructive measure gives snapshots of the atom distribution in the space. We examine in the following whether it is possible to extract information about the atom dynamics from this type of measurement.

3. Dynamics of atoms inside the wells

Before we search for signatures of the dynamics in the experimental measurements, let us investigate in more detail what are the relevant parameters and characteristics of the atom dynamics in a lattice. To illustrate this approach, let us consider again the two lattices introduced in §2. Although these two lattices differ only by the sign of their potential, they are very different. U_- has its wells where the light intensity is maximum, while U_+ has its wells where the intensity vanishes. Let us denote by E_T the value of the potential energy at the saddle point of the intensity. Atoms, the energy E of which is smaller than the threshold E_T , are trapped into one site because they cannot climb up to the saddle point. On the contrary, atoms with $E > E_T$ can travel between sites, if they move in the right direction.

Inside a trap site, the energy of the atom plays the role of a stochastic parameter. Indeed, for low energies, the atoms remain located close to the bottom of the well, and their dynamics can be approximated by a harmonic motion. As the energy increases, the potential becomes more anharmonic, the nonlinearities increase and the dynamics can become more complex. To be able to compare the behaviour of atoms in different potentials, we take, in the following, the origin of the energy at the bottom of the wells and normalize the energy so that $E_T = 1$. The potential energy then takes a different form for red and blue detunings

$$U_+ = \frac{I}{1 - \alpha^2} \quad (3.1)$$

and

$$U_- = \frac{2(1 + \alpha) - I}{(1 + \alpha)^2}. \quad (3.2)$$

Let us now examine in detail the dynamics of the atoms in our two potentials. The most relevant way is to look at the evolution of the Poincaré sections as a function of the energy. Our phase space is four-dimensional, with directions (X, Y, \dot{X}, \dot{Y}) , but, because of the energy conservation, the accessible space reduces to a three-dimensional surface. We choose to consider the Poincaré section at $\dot{Y} = 0$ with increasing values, and, thus, Poincaré sections are in the three-dimensional space (X, Y, \dot{X}) , and they lie on a two-dimensional surface S_P , which is shaped like a semi-ellipsoid. To represent the Poincaré sections, we can project them on the (X, Y) plane or on the more usual (X, \dot{X}) plane. The latter shows the Poincaré sections viewed from the vertex of the semi-ellipsoid. However, here, because of the stiff sides of S_P , the projection in this plane leads to a confused map, as many curves are projected at the same location, and thus are superimposed. On the contrary, the projection on the (X, Y) plane gives more detail, and thus, in the following, we often choose it. However, let us keep in mind that we are looking at the lateral projection of a ‘bell’, and thus that we superimpose its front and rear faces.

As pointed out before, because of the normalization we choose for the energy, the form of the potential energy differs in the cases of blue or red detuned lasers. We investigate each case separately.

In the case of red detuned lasers, the potential energy takes the form

$$U_- = \omega_0^2(1 - \cos X) + \omega_0^2(1 - \cos Y) - \frac{(1 - \cos X)(1 - \cos Y)}{(1 + \alpha)^2} \quad (3.3)$$

with

$$\omega_0^2 = (1 + \alpha)^{-1}. \quad (3.4)$$

This potential appears to be the sum of two simple pendula coupled through the third term. The frequency for oscillations with a small amplitude is the same for the two directions. This degeneracy, together with the coupling term, leads to a strong synchronization of the motion in the two directions (Bennett *et al.* 2002). However, in contrast with the Huygens clocks, we do not have any dissipation here, and so the frequency locking occurs in a more subtle way (Hennequin & Verkerk *in press*).

It is interesting to identify the resonances of the system. A very simple approach is to restrict the problem to the first anharmonic terms, similar to the undamped Duffing oscillator. We then look for a periodic harmonic solution in the form $X = X_0 \cos(\omega t)$ and $Y = Y_0 \cos(\omega t + \varphi)$, with ω close to ω_0 . We drop terms at other frequencies (i.e. 3ω) and, consequently, have six families of solutions. The first two are the trivial ones—motion along the X or the Y directions ($Y_0 = 0$ or $X_0 = 0$). The other four are obtained for $X_0 = Y_0$ and for $\varphi = 0, \pi, \pm\pi/2$. For a given energy E , the relations giving X_0 and ω are not simple, and it is beyond the aim of this article to write them explicitly. For the large amplitudes considered in the following, the motion is no longer harmonic and we cannot keep only the lower order terms, but the main result remains—we have six periodic trajectories, leading to points in the Poincaré section (except for the trajectory $Y_0 = 0$, which we cannot catch in a Poincaré section at $\dot{Y} = 0$). In the three-dimensional space, these points have the coordinates $(0, -Y_0, 0)$, $(\pm X_0, -X_0, 0)$ and $(0, -X'_0, \pm\omega X'_0)$.

In figure 2, we show the dynamics in the U_- potential for different normalized energies in the case of $\alpha = 0.5$. These results have been obtained through numerical resolution of the equations of motion that are derived from the potential (3.3), without the addition of any random quantity. All the described behaviours are thus deterministic. For each value of the energy, we project the Poincaré section on the (X, Y) plane (figure 2*a,c,e*) and on the (X, \dot{X}) plane (figure 2*b,d,f*). For low enough energies (e.g. $E = 0.8$, figure 2*a,b*), we see four distinct domains separated by an X-shaped separatrix. In each of these domains, the Poincaré section is cycling around one of the non-trivial resonances found above. As the motion along X and Y is governed by the same frequency, and because of the coupling between these two pendula, a synchronization between the two directions occurs, through a phase locking between the two motions. The corresponding behaviour can be described as mainly a ω periodic cycle perturbed by small sidebands (Hennequin & Verkerk in press).

The dynamics in U_- evolves only slightly when E is increased. The Poincaré surfaces are always organized around the separatrix delimiting four areas. In each area, the nature of the motion is the same, namely phase locking between the motions in the X and Y directions. Chaos appears close to the separatrix for $E \simeq 0.88$ (figure 2*c,d*), but it remains marginal, even when $E = 1$ (figure 2*e,f*). This very small extent is due to the original degeneracy of the frequencies of the coupled pendula and to the strong coupling between them (Hennequin & Verkerk in press).

For blue detunings ($\Delta > 0$), the bottom of the well corresponds to $I = 0$, i.e. $(X = 0, Y = \pi)$ sites. For the sake of simplicity, we shift the origin in Y by π , in order to have a trapped motion centred at the origin. Thus, we can write

$$U_+ = \omega_{0X}^2(1 - \cos X) + \omega_{0Y}^2(1 - \cos Y) - \frac{(1 - \cos X)(1 - \cos Y)}{(1 - \alpha^2)} \quad (3.5)$$

with

$$\omega_{0X}^2 = (1 + \alpha)^{-1} \quad (3.6)$$

and

$$\omega_{0Y}^2 = (1 - \alpha)^{-1}. \quad (3.7)$$

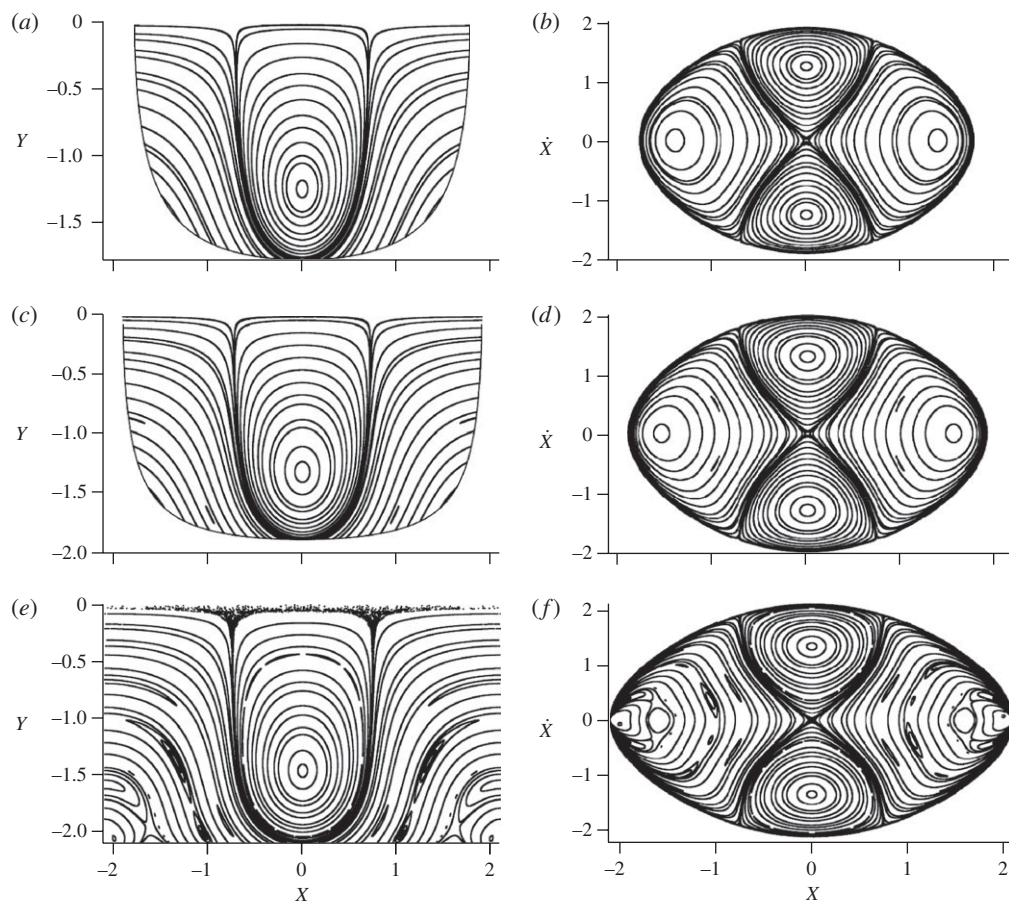


Figure 2. (a, c, e) (X, Y) and (b, d, f) (X, \dot{X}) Poincaré sections of the atomic dynamics in the U_- potential. (a, b) $E = 0.80$; (c, d) $E = 0.88$; (e, f) $E = 1.00$.

Once again, this potential appears to be the sum of two coupled pendula. But, now, the two frequencies for oscillations with small amplitudes are different—for the value $\alpha = 0.5$ chosen here, the ratio $\sqrt{3}$ of these two frequencies is irrational.

For very small energies (figure 3*a*), the dynamics consists essentially of a regular motion around the bottom of the well, along a quasi-periodic trajectory with frequencies ω_X and ω_Y close to ω_{0X} and ω_{0Y} . At the top of figure 3*a*, Poincaré sections are those of atoms, the motion of which is essentially along the X -axis. In $Y = 0$, the trajectory is a periodic cycle along the X direction (edge of the semiellipsoid). On the contrary, the periodic cycle at the bottom of the figure corresponds to the situation where the atomic motion is exclusively along the Y -axis (vertex of the semiellipsoid). Note that the nature of the motion along these quasi-periodic cycles is very different from those described with $\Delta < 0$. Indeed, as ω_{0X} and ω_{0Y} are very different, no locking occurs. In particular, in the spectrum of the motion, the two main frequencies are close to ω_{0X} and ω_{0Y} .

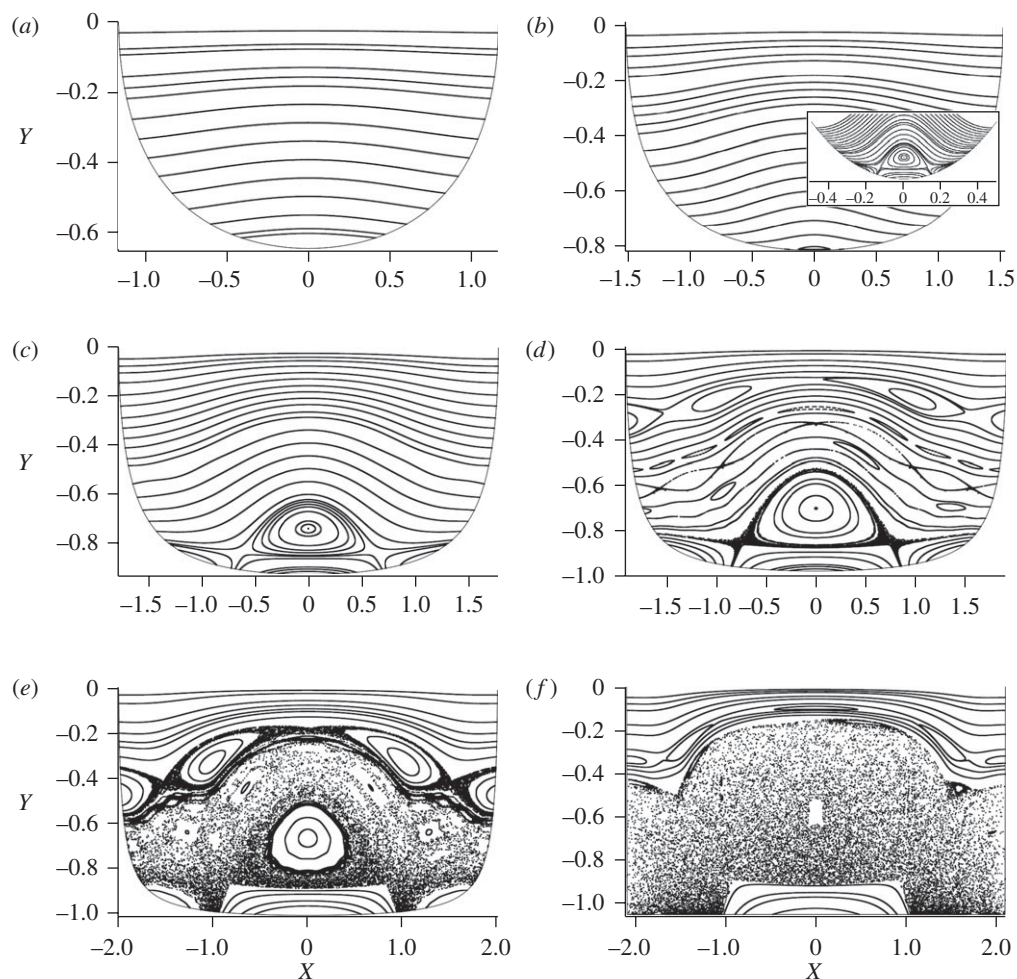


Figure 3. (X, Y) Poincaré sections of the atomic dynamics in the U_+ potential. (a) $E = 0.4$, (b) $E = 0.63$, (c) $E = 0.80$, (d) $E = 0.88$, (e) $E = 0.93$ and (f) $E = 1.00$.

As the energy of the atom is increased, the atom can climb further and further in the well, the frequencies ω_X and ω_Y change because of the anharmonicity of the potential, but the dynamics does not change fundamentally until $E \simeq 0.6$. At that point, a new feature appears—a stable periodic trajectory shows up as a cycle close to the bottom of figure 3b, obtained for $E = 0.63$. In fact, for amplitudes large enough, the frequencies ω_X and ω_Y depart so much from their initial values ω_{0X} and ω_{0Y} that a new resonance appears at $\omega_Y = 2\omega_X$.

For higher energies, the $\omega_Y = 2\omega_X$ resonance grows and comes closer to the centre of the figure and influences a non-negligible fraction of the trajectories. In figure 3c, for $E = 0.8$, the resonance is clearly visible in $Y \simeq -0.74$. In the (X, Y, \dot{X}) space, its Poincaré section consists of two points (superimposed in the projection of figure 3c), explored alternatively by the trajectory. Around this point, the Poincaré sections are a double closed loop. The corresponding

quasi-periodic motion consists of a perturbed $\omega_Y = 2\omega_X$ phase-locked periodic cycle, where the perturbation consists of small sidebands of ω_X and ω_Y in the spectrum. Thus, the separatrix appears here to be the limit between this phase-locked and the unlocked behaviours. The central domain and the two linked lateral domains (figure 3*e,f*) correspond to the phase locking. The difference between these two domains is the relative phase on the motion along X and Y . In the two other domains (top and bottom), there is no locking between the ω_X and ω_Y frequencies.

In $E = 0.8$ (figure 3*c*), all the trajectories are still periodic cycles or quasi-periodic tori. When the energy is increased further, chaos appears at $E \simeq 0.88$, starting in the vicinity of the separatrix (figure 3*d*). Then, it expands with some quasi-periodic islands remaining (figure 3*e*), but finally, for $E = 1$ (figure 3*f*), the only significant quasi-periodic domains are those around the X and Y periodic cycles. Around the locked periodic cycles, a narrow area with tori remains, but chaos appears really to be dominant.

We have shown in this section that it is relatively easy to find two slightly different lattices with fundamentally different dynamics. These two configurations are easy to reach experimentally, as they differ only by the sign of the detuning. It would be interesting now to examine how to measure experimentally these differences, and whether these differences have an impact on the dynamics of atoms when they jump between sites of the lattice. The next section deals with the latter.

4. Dynamics of atoms visiting several wells

To travel from site to site, an atom needs to have an energy $E \geq 1$, but this is not a sufficient condition. Only atoms with an adequate trajectory will effectively escape from a well. This implies that, for a given energy $E \geq 1$, at least two classes of atoms can exist—trapped atoms remaining in a single well, and travelling atoms, which escape the wells. In fact, the situation is more complex, as we will see now.

Let us first examine the dynamics of travelling atoms in the blue case ($\Delta > 0$). We are interested here in atoms with an energy $1 < E < 4$. Indeed, atoms with $E > 4$ have an energy larger than the potential maximum, and thus they ‘fly’ above the potential, and their trajectory is purely ballistic. On the contrary, the dynamics of the atoms with an intermediate energy consists of complex trajectories visiting a large number of sites, as in a random walk. As our model is fully deterministic, it involves, in fact, chaotic trajectories. Figure 4*a* illustrates such a chaotic diffusion—it reports the trajectories followed by 100 atoms. Such a trajectory is in fact an alternation of oscillations inside wells and of jumps between wells. Here, we know that chaos dominates inside the wells, and thus the chaotic nature of the diffusion is not surprising. However, as we will see below, the existence of chaos inside the wells is not a necessary condition to observe a chaotic diffusion.

To think of an experimental characterization of this chaotic diffusion, a simple way would be to characterize the diffusion function and to evaluate a diffusion coefficient. Figure 5*a* shows the distance covered by atoms of high energy ($E = 2.66$) as a function of time. With such high energies, all atoms travel between

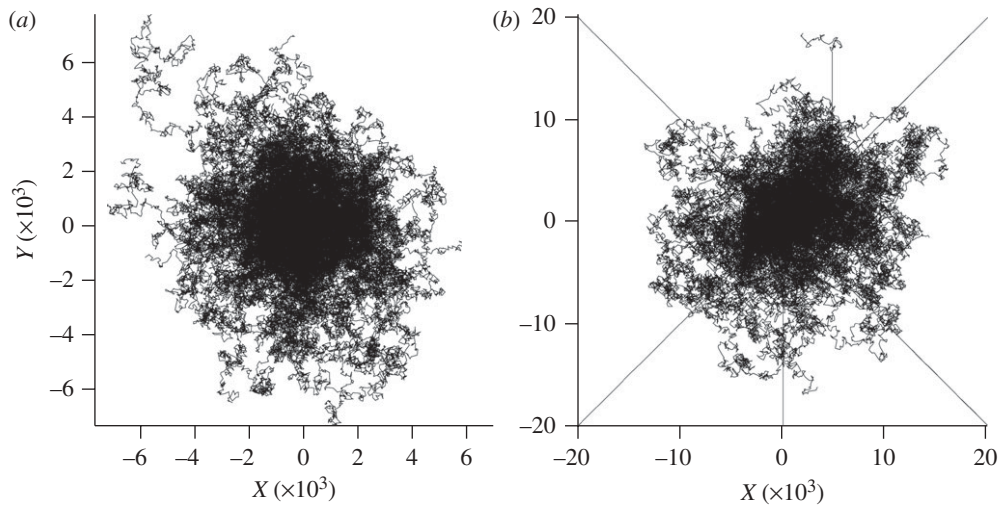


Figure 4. (X, Y) plot of the trajectories of 100 atoms in the (a) U_+ ($E = 2.66$) and (b) U_- ($E = 1.07$) lattices. Each atom starts in the central mesh, and moves during the time $t = 10^6$, which corresponds to more than 10^5 periods of oscillation at the bottom of a well.

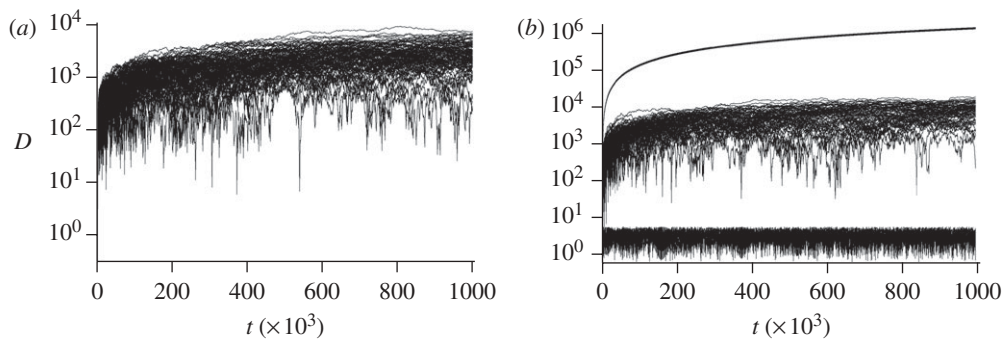


Figure 5. Distance covered by 100 atoms as a function of time. Parameters are the same as in figure 4: (a) U_+ and $E = 2.66$; (b) U_- and $E = 1.07$.

wells. They all follow a similar behaviour, characterized by a diffusion over a distance of the order of 10^3 for the time interval of the figure. Although there is a small dependence of these curves as a function of the energy of the atom, the orders of magnitude remain the same for all energies $1 < E < 4$. The only difference is that, for lower energies, some atoms remain trapped in their well, and so a second group of curves appears with atoms remaining within a short distance (smaller than the mesh, i.e. 2π) of their initial location.

In the red detuned situation ($\Delta < 0$), the maximum of the potential is at $E = 1.33$. As in the blue case, atoms with an energy $E > 1.33$ have ballistic trajectories, and atoms with $1 < E < 1.33$ exhibit a diffusive chaotic behaviour (Figure 4b). The origin of chaos now is clearly in the jumps between wells, as the dynamics in the wells is regular. And, in fact, there is a main difference when compared

with the blue case—the diffusion scale is larger by one order of magnitude, on the whole interval $1 < E < 1.33$. We did not check whether the slower diffusion originates effectively in the chaotic trajectories followed by the atoms inside the wells, but it would be interesting to check in a future study how these chaotic behaviours could slow down the atoms. However, the difference of one order of magnitude in the diffusion speed reveals that the macroscopic behaviour of atoms could effectively be used to characterize the nature of the dynamics in optical lattices.

But there is another important difference between the two lattices—in the red case, a third regime exists, neither trapping nor diffusing. This is illustrated in figure 4*b*, where trajectories appear following the two bisectors. These trajectories correspond to atoms travelling along the escape lines of the lattice, as they were described in §2. These atoms follow, in fact, a ballistic trajectory, where they travel very rapidly along the bisectors. For example, in figure 4*b*, the ballistic trajectories reach 10^6 in all directions, while the diffusive atoms reach only 2×10^4 of the same units in the same time. Note that the ballistic trajectories we discuss here occur as soon as the threshold $E = 1$ is reached, and only along the escape lines of the potential.

Figure 5*b* shows the distance covered by the atoms as a function of time. We now clearly have three groups of trajectories: trapped trajectories at the bottom, diffusive trajectories for distances of about 10^4 and ballistic trajectories at the top, for distances larger than 10^5 . The main difference when compared with the $\Delta > 0$ case is the cohabitation of ballistic and diffusive trajectories, even just above the threshold. This provides evidence of three specific time scales of the dynamics of atoms with a given energy, associated, respectively, with the trapped, the chaotic diffusive and the ballistic trajectories.

In this section, we examined the dynamics of atoms, whose energy is large enough to escape the potential wells, but remains smaller than the potential maxima. We focused on atoms travelling between wells, and found a different behaviour for our two lattices. For the red lattice, atoms can be classified according to two types of dynamics—the diffusive atoms exhibit a chaotic dynamics carrying them off their initial location; the ballistic atoms move away rapidly from their initial location. These behaviours are associated with two different time scales. But is it sufficient to identify these different regimes in a real experiment? We have also shown that the dynamics of atoms in the blue lattice is quite different, both for the diffusive regime and for the ballistic one—the time scale of the former is one order of magnitude smaller, while the latter simply does not exist. Can we use these properties to characterize and distinguish experimentally the two lattices? These questions are discussed in the next section.

5. Macroscopic signatures of chaos

Our aim is to characterize the dynamics of the cold atoms in the optical lattice. As we are concerned by conservative lattices, we cannot hope to ‘film’ in real time the atoms in the lattice, as it would introduce dissipation. Thus, we have to find other techniques. As the specificity of each lattice concerns the travelling atoms, an experimental measurement aimed at characterizing these lattices should characterize these travelling atoms.

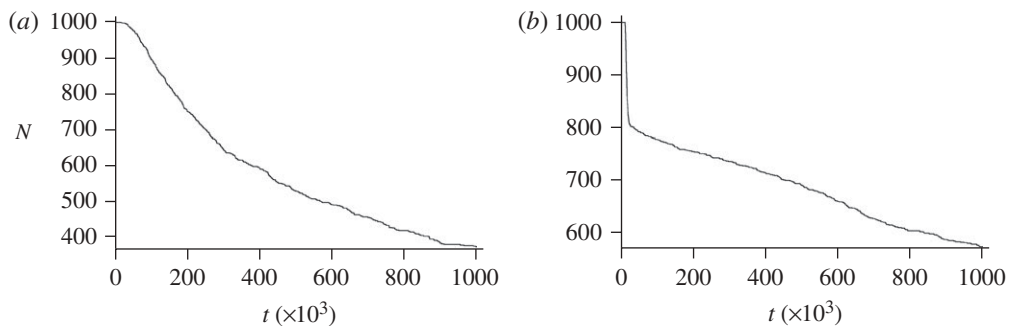


Figure 6. Number of atoms versus time in (a) U_+ potential and (b) U_- potential.

Experimentally, the lattice is finite. So the travelling atoms will reach the edge of the lattice, and finally leave the lattice. Therefore, a simple measure of the lifetime of the atoms in the lattice gives information about the trapped and travelling atoms. However, as there are several types of travelling atoms, the simple measure of a lifetime is not sufficient, and the lifetime curve itself, in particular its shape, must be analysed. Thus, we will plot now the number of atoms in the lattice as a function of time. The shape of the curve and the lifetime itself should give information about the travelling atoms, while the baseline gives the percentage of trapped atoms.

In the experiment, all the atoms do not have the same energy, but, on the contrary, they exhibit a distribution of energies linked to their temperature. Thus, the results shown below have been obtained by using a sample of atoms with an appropriate distribution of energy.

Figure 6a shows the number of atoms in the blue lattice versus time. To simulate the finite size of the lattice, atoms are removed as soon as they reach a distance $D_L = 1000$. The curve exhibits a plateau at short times, followed by an exponential-like decrease to an asymptote. The plateau corresponds to the time needed by the first atoms to reach the edge of the lattice (in the simulations, all the atoms are supposed to be initially at the centre of the lattice). The decrease corresponds to the diffusing atoms escaping the lattice, and the asymptote to the number of atoms trapped in wells. This behaviour does not depend on the lattice size D_L , except that the lifetime of atoms increases. In fact, the distance $D_L = 1000$, i.e. about 150 lattice meshes or $70 \mu\text{m}$ for a Cs trap, is smaller by one order of magnitude than a typical experimental result. However, a value of $D_L = 10^4$ leads, for the data presented in figures 4a and 5a, to an almost flat curve because the time series are not long enough. To reach such a distance, one should increase the evolution time by two orders of magnitude.

Figure 6b shows the number of atoms in the red lattice versus time, for $D_L = 10^4$. The shape of the curve is qualitatively different from that obtained for the blue lattice. At short times, a fast decrease appears, corresponding to the loss of the ballistic atoms. At long times, not visible in the figure, an asymptote is reached, corresponding to the trapped atoms. The intermediate decrease corresponds to the loss of the diffusing atoms. Note that the decrease appears to be more or less linear. In fact, the shape of this part of the curves

is the sum of the diffusing losses of different classes of atoms differing by their energy. As a function of D_L , this sum can exhibit very different shapes, from an exponential-like shape, as in figure 6*a*, to an almost linear shape, as in figure 6*b*.

Figure 6 shows that the measure of the lifetime of atoms in a conservative optical lattice provides qualitative and quantitative information about the nature of the lattice and the nature of the dynamics of the atoms in the lattice, in particular about the chaotic diffusion. Therefore, the measure of the atom lifetime, in particular the existence of several characteristic times in the decrease of the atom number, appears to be a signature of the chaotic dynamics of atoms in the lattice.

6. Conclusion

We have shown in this paper that optical lattices are a good toy model to study experimentally the dynamics of conservative systems, provided that relevant experimental measures are found to characterize this dynamics. In particular, we show that changing a simple experimental parameter can lead to two very different lattices, where atoms exhibit very different dynamical behaviours. We have shown that these differences exist both in the local dynamics of atoms inside a well and in the non-local dynamics of atoms travelling between wells. We searched numerically for signatures of these different dynamics in the experimentally accessible quantities, and found that the measure of atom lifetimes in the lattice gives vast information about the existence and the type of chaotic diffusion of the atoms.

It would be interesting now to characterize more precisely the diffusion function, as a function of the experimental parameters, in particular the atom temperature and the lattice size, and obviously to test these results in a real experiment.

We considered in this paper only the dynamics of classical atoms, and it appears that this dynamics is more complex and more subtle than those usually considered. Simple statistical analyses are not enough to fully characterize this dynamics, and more suitable tools are necessary. It is important now to think about the consequences of these results in the quantum regime, and, in particular, about what the equivalent measures could be in the quantum world.

We thank Frédéric Carlier for fruitful discussions. The Laboratoire de Physique des Lasers, Atomes et Molécules is Unité Mixte de Recherche de l'Université de Lille 1 et du CNRS (UMR 8523). The Centre d'Études et de Recherches Lasers et Applications (CERLA) is supported by the Ministère chargé de la Recherche, the Région Nord-Pas de Calais and the Fonds Européen de Développement Économique des Régions.

References

- Bennett, M., Schatz, M. F., Rockwood, H. & Wiesenfeld, K. 2002 Huygens' clocks. *Proc. R. Soc. Lond. A* **458**, 563–579. (doi:10.1098/rspa.2001.0888)
- Billy, J. *et al.* 2008 Direct observation of Anderson localization of matter waves in a controlled disorder. *Nature* **453**, 891–894. (doi:10.1038/nature07000)
- Chabé, J., Lemaire, G., Gremaud, B., Delande, D., Szriftgiser, P. & Garreau, J. C. 2008 Experimental observation of the Anderson metal-insulator transition with atomic matter waves. *Phys. Rev. Lett.* **101**, 255 702. (doi:10.1103/PhysRevLett.101.255702)

- Courtade, E., Houde, O., Clément, J.-F., Verkerk, P. & Hennequin, D. 2006 Dark optical lattice of ring traps for cold atoms. *Phys. Rev. A* **74**, 031 403(R). (doi:10.1103/PhysRevA.74.031403)
- di Stefano, A., Fauquembergue, M., Verkerk, P. & Hennequin, D. 2003 Giant oscillations in the magneto-optical trap. *Phys. Rev. A* **67**, 033 404. (doi:10.1103/PhysRevA.67.033404)
- di Stefano, A., Verkerk, P. & Hennequin, D. 2004 Deterministic instabilities in the magneto-optical trap. *Eur. Phys. J. D* **30**, 243–258. (doi:10.1140/epjd/e2004-00089-y)
- Douglas, P., Bergamini, S. & Renzoni, F. 2006 Tunable tsallis distributions in dissipative optical lattices. *Phys. Rev. Lett.* **96**, 110 601. (doi:10.1103/PhysRevLett.96.110601)
- Fang, J. & Hai, W. 2005 Wannier–Stark chaos of a Bose–Einstein condensate in 1D optical lattices. *Physica B* **370**, 61–72. (doi:10.1016/j.physb.2005.08.033)
- Greiner, M., Bloch, I., Mandel, O., Hänsch, T. W. & Esslinger, T. 2001 Exploring phase coherence in a 2D lattice of Bose–Einstein condensates. *Phys. Rev. Lett.* **87**, 160 405. (doi:10.1103/PhysRevLett.87.160405)
- Greiner, M., Mandel, O., Esslinger, T., Hänsch, T. W. & Bloch, I. 2002 Quantum phase transition from a superfluid to a Mott insulator in a gas of ultracold atoms. *Nature* **415**, 39–44. (doi:10.1038/415039a)
- Guidoni, L. & Verkerk, Ph. 1999 Optical lattices: cold atoms ordered by light. *J. Opt. B Quantum Semicl. Opt.* **1**, R23–R45.
- Guidoni, L., Triche, C., Verkerk, P. & Grynberg, G. 1997 Quasiperiodic optical lattices. *Phys. Rev. Lett.* **79**, 3363–3366. (doi:10.1103/PhysRevLett.79.3363)
- Guidoni, L., Depret, B., di Stefano, A. & Verkerk, P. 1999 Atomic diffusion in an optical quasicrystal with five-fold symmetry. *Phys. Rev. A* **60**, R4233–R4236. (doi:10.1103/PhysRevA.60.R4233)
- Hennequin, D. 2004 Stochastic dynamics of the magneto-optical trap. *Eur. Phys. J. D* **28**, 135–147. (doi:10.1140/epjd/e2003-00293-3)
- Hennequin, D. & Verkerk, P. In press. Synchronization in non dissipative optical lattices. *Eur. Phys. J. D*. (doi:10.1140/epjd/e2009-00324-1)
- Jaksch, D. & Zoller, P. 2005 The cold atom Hubbard toolbox. *Ann. Phys.* **315**, 52–79. (doi:10.1016/j.aop.2004.09.010)
- Jersblad, J., Ellmann, H., Stchkel, K., Kastberg, A., Sanchez-Palencia, L. & Kaiser, R. 2004 Non-Gaussian velocity distributions in optical lattices. *Phys. Rev. A* **69**, 013 410. (doi:10.1103/PhysRevA.69.013410)
- Kuan, W. H., Jiang T. F. & Cheng, S. C. 2007 Instabilities of Bose–Einstein condensates in optical lattices. *Chin. J. Phys.* **45**, 219.
- Lignier, H., Chabé, J., Delande, D., Garreau, J. C. & Szriftgiser, P. 2005 Reversible destruction of dynamical localization. *Phys. Rev. Lett.* **95**, 234 101. (doi:10.1103/PhysRevLett.95.234101)
- Mandel, O., Greiner, M., Widera, A., Rom, T., Hänsch, T. W. & Bloch, I. 2003 Controlled collisions for multi-particle entanglement of optically trapped atoms. *Nature* **425**, 937–940. (doi:10.1038/nature02008)
- Paredes, B., Widera, A., Murg, V., Mandel, O., Fölling, S., Cirac, I., Shlyapnikov, G. V., Hänsch, T. W. & Bloch, I. 2004 Tonks-Girardeau gas of ultracold atoms in an optical lattice. *Nature* **429**, 277–281. (doi:10.1038/nature02530)
- Roati, G., D’Errico, C., Fallani, L., Fattori, M., Fort, C., Zaccanti, M., Modugno, G., Modugno, M. & Inguscio, M. 2008 Anderson localization of a non-interacting Bose–Einstein condensate. *Nature* **453**, 895–898. (doi:10.1038/nature07071)
- Steck, D. A., Milner, V., Oskay, W. H. & Raizen, M. G. 2000 Quantitative study of amplitude noise effects on dynamical localization. *Phys. Rev. E* **62**, 3461–3475. (doi:10.1103/PhysRevE.62.3461)
- Thommen, Q., Garreau, J. C. & Zehnlé, V. 2003 Classical chaos with Bose–Einstein condensates in tilted optical lattices. *Phys. Rev. Lett.* **91**, 210 405. (doi:10.1103/PhysRevLett.91.210405)
- Vollbrecht, K. G. H., Solano, E. & Cirac, J. I. 2004 Ensemble quantum computation with atoms in periodic potentials. *Phys. Rev. Lett.* **93**, 220 502. (doi:10.1103/PhysRevLett.93.220502)
- Wilkowski, D., Ringot, J., Hennequin, D. & Garreau, J. C. 2000 Instabilities in a magneto-optical trap: noise-induced dynamics in an atomic system. *Phys. Rev. Lett.* **85**, 1839–1842. (doi:10.1103/PhysRevLett.85.1839)